

Compressed Representation of Kohn–Sham Orbitals via Selected Columns of the Density Matrix

Anil Damle,^{*,†} Lin Lin,^{‡,§} and Lexing Ying^{†,∇}

[†]Institute for Computational and Mathematical Engineering, Stanford University, Stanford, California, United States

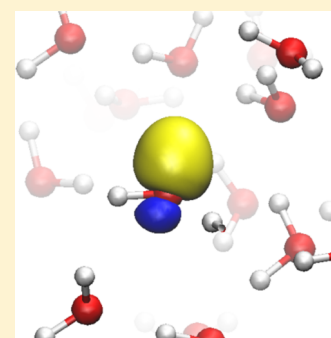
[‡]Department of Mathematics, University of California, Berkeley, Berkeley, California, United States

[§]Computational Research Division, Lawrence Berkeley National Laboratory, Berkeley, California, United States

[∇]Department of Mathematics, Stanford University, Stanford, California, United States

Supporting Information

ABSTRACT: Given a set of Kohn–Sham orbitals from an insulating system, we present a simple, robust, efficient, and highly parallelizable method to construct a set of optionally orthogonal, localized basis functions for the associated subspace. Our method explicitly uses the fact that density matrices associated with insulating systems decay exponentially along the off-diagonal direction in the real space representation. We avoid the usage of an optimization procedure, and the localized basis functions are constructed directly from a set of selected columns of the density matrix (SCDM). Consequently, the core portion of our localization procedure is not dependent on any adjustable parameters. The only adjustable parameters present pertain to the use of the SCDM after their computation (for example, at what value should the SCDM be truncated). Our method can be used in any electronic structure software package with an arbitrary basis set. We demonstrate the numerical accuracy and parallel scalability of the SCDM procedure using orbitals generated by the Quantum ESPRESSO software package. We also demonstrate a procedure for combining the orthogonalized SCDM with Hockney’s algorithm to efficiently perform Hartree–Fock exchange energy calculations with near-linear scaling.



1. INTRODUCTION

Kohn–Sham density functional theory (KSDF) is the most widely used electronic structure theory for molecules and systems in condensed phase. In KSDF, the many-body electronic structure properties are, in principle, exactly mapped into a fictitious single-particle system. The Kohn–Sham orbitals, which are orthonormal eigenfunctions of the single particle Kohn–Sham Hamiltonian operator, can describe various physical quantities, such as density, energy, and atomic forces. However, it is expensive to compute and store the Kohn–Sham orbitals of large systems, which are spatially delocalized. Let N be the number of degrees of freedom and N_e be the number of electrons in the system. The cost for storing the Kohn–Sham orbitals is $O(NN_e)$, and the cost for computing them is generally $O(NN_e^2)$, or “cubic scaling”, assuming $N \approx O(N_e)$. In modern KSDF calculations, the Hartree–Fock exact exchange term is also often taken into account in the form of hybrid functionals.^{3,4} The computational cost for this step not only scales cubically but also has a large preconstant, which limits the application of hybrid functional calculations to hundreds of atoms.

In order to reduce both the storage requirements and the cost associated with subsequent computations, it is important to realize that the Kohn–Sham orbitals are not unique. Any nondegenerate linear transformation of the set of Kohn–Sham orbitals yields exactly the same physical properties of a system. In other words, the physically relevant quantity is the subspace

spanned by the Kohn–Sham orbitals. Various efforts^{5–10} have been made to utilize this fact and to find a set of localized orbitals that form a compressed representation of a Kohn–Sham subspace. For example, the Boys localization⁵ and, subsequently, the Marzari–Vanderbilt^{6,7} construction of maximally localized Wannier functions (MLWFs) uses a nonlinear optimization approach to find a unitary transformation of the Kohn–Sham subspace into a set of orthogonal functions localized in real space. The locality, or the “nearsightedness” principle, is guaranteed for insulating systems with a finite HOMO–LUMO gap.^{11,12} The localized orbitals have wide applications in chemistry and physics. For instance, localized orbitals can be used to construct linear scaling methods for solving KSDF using local and semilocal functionals,^{13,14} and for calculations using hybrid functionals.^{15,16}

In this manuscript, we present an alternative method to the widely used MLWFs to compute a set of localized orbitals associated with the Kohn–Sham subspace for insulating systems. Our method is simple, robust, efficient, and highly parallelizable. We explicitly use the fact that for insulating systems the single particle density matrix is exponentially localized along the off-diagonal direction in the real-space representation.^{11,17–21} Our algorithm finds a set of localized

Received: November 3, 2014

orbitals by directly using selected columns of the density matrix (SCDM) associated with the Kohn–Sham orbitals. Consequently, by construction the SCDM are localized in the real space representation. As opposed to the MLWFs which are orthonormal, the SCDM are not orthonormal in general. However, a set of orthonormal and localized functions spanning the Kohn–Sham subspace can be obtained via a simple linear transformation of the SCDM.

In contrast with Boys localized orbitals or MLWFs, our method does not attempt to minimize a given localization criteria via a minimization procedure. Consequently, our method does not require any initial guess of localized orbitals, is of fixed cost for a given problem size, and avoids some of the potential problems of a minimization scheme, such as getting stuck at a local minimum. In fact, our method should be more robust than an iterative minimization procedure for finding localized orbitals. The locality of the SCDM is a direct consequence of the locality of the density matrix, and is comparable to that obtained from the MLWF procedure. Furthermore, the localization procedure we present is not explicitly dependent on any adjustable parameters. Rather, the only adjustable parameter we later discuss is the truncation threshold to subsequently apply to our computed localized functions. Finally, if desired, the SCDM and MLWF procedures could be combined, since the orthogonalized SCDM should already be a very good initial guess for an optimization-based approach.

Our method can be used in any electronic structure software package with any basis set, ranging from planewaves to Gaussian basis sets, provided that the Kohn–Sham orbitals can be represented on a real space grid. One striking feature of our method is its simplicity: a prototype sequential implementation takes just a few lines of code. The construction of the SCDM only involves simple linear algebra routines such as a rank-revealing QR factorization and matrix–matrix multiplication. Therefore, the parallel implementation for computing the SCDM can straightforwardly scale, for the problem size we tested, to more than 1000 processors. This enables the computation of localized basis functions for the self-consistent treatment of the Hartree–Fock terms in KSDFT calculations with hybrid exchange–correlation functionals.

As an application, we also demonstrate a procedure for combining the orthogonalized SCDM with Hockney’s algorithm to efficiently compute the Hartree–Fock exchange energy.

2. THEORY

For insulating systems, the locality of the single particle density matrix along the off-diagonal direction generally can be observed in the real-space representation.^{11,12} For the sake of clarity, in this manuscript, we explicitly require the Kohn–Sham orbitals to be represented on a real space grid defined as below. In some cases, the real-space representation may not be necessary, and we postpone such a discussion to the conclusion.

Let $\{\psi_j(x)\}_{j=1}^{N_e}$ be a set of Kohn–Sham orbitals that satisfy the orthonormality condition

$$\int \psi_j^*(x) \psi_j(x) dx = \delta_{jj}, \quad (1)$$

and we have access to $\psi_j(x)$ evaluated at a set of discrete grid points $\{x_i\}_{i=1}^N$. Let $\{\omega_i\}_{i=1}^N$ be a set of positive integration weights associated with the grid points $\{x_i\}_{i=1}^N$, then the discrete orthonormality condition corresponding to eq 1 is given by

$$\sum_{i=1}^N \psi_j(x_i) \psi_j(x_i) \omega_i = \delta_{jj}, \quad (2)$$

Let $\Psi_j = [\psi_j(x_1), \psi_j(x_2), \dots, \psi_j(x_N)]^T$ be a column vector, and $\tilde{\Psi} = [\Psi_1, \dots, \Psi_{N_e}]$ be a matrix of size $N \times N_e$. In this paper, we call $\tilde{\Psi}$ the *real-space representation* of the Kohn–Sham orbitals. We also define a diagonal matrix $W = \text{diag}[\omega_1, \dots, \omega_N]$.

It should be noted that the real-space representation of Kohn–Sham orbitals can be obtained with any type of basis set; therefore, our method is applicable for any electronic structure software package. For instance, if the Kohn–Sham orbitals are represented using the planewave basis functions, their real-space representation can be obtained on a uniform grid efficiently with the fast Fourier transform (FFT) technique. In such case, the parameter ω_i takes the same constant value for all i . For general basis sets such as Gaussian basis functions or localized atomic orbitals, let $\{\chi_k(x)\}_{k=1}^M$ be the collection of basis functions (usually $M \ll N$). We first evaluate each basis function on the real-space grid as $\chi_k = [\chi_k(x_1), \chi_k(x_2), \dots, \chi_k(x_N)]^T$, and denote by $X = [\chi_1, \dots, \chi_M]$ the collection of all basis functions, where X is a matrix of size $N \times M$. The Kohn–Sham orbitals then can be obtained as the linear combination of basis functions as $\tilde{\Psi} = XZ$. Here, the matrix Z of size $M \times N_e$ and is usually obtained by solving a generalized eigenvalue problem. For these general basis functions and, in particular, in all-electron calculations, the grid points are usually chosen to be nonuniform to improve the accuracy of numerical quadrature; correspondingly, the weight parameters ω_i also are nonuniform.

We define $\Psi = W^{1/2} \tilde{\Psi}$ to be the set of weighted Kohn–Sham orbitals represented in the real space, in which case the discrete orthonormality condition in eq 2 becomes $\Psi^* \Psi = I$, where I is an identity matrix of size N_e . We now seek a compressed basis for the span of Ψ , denoted by the set of vectors $\Phi = [\phi_1, \dots, \phi_{N_c}]$, such that each ϕ_i is localized. The single particle density matrix is defined as $P = \Psi \Psi^*$. The nearsightedness principle states that, for insulating systems, each column of the matrix P is localized. As a result, selecting any linearly independent subset of N_e of them will yield a localized basis for the span of Ψ . However, picking N_e random columns of P may result in a poorly conditioned basis if, for example, there is too much overlap between the selected columns. Therefore, we would like a means for choosing a well-conditioned set of columns, denoted as C , to use as the localized basis. Intuitively, we expect such a basis to select columns to minimize overlaps with each other when possible.

To achieve this we utilize the so-called *interpolative decomposition*.²² Given an $N \times N$ matrix A with rank k , such a factorization seeks to find a permutation matrix Π , a subset of k columns of A whose indices form the set C and a matrix T such that

$$A \Pi = A_{:,C} [I \ T] \quad (3)$$

and $\|T\|$ should be small. The interpolative decomposition can be computed via the (strong) rank revealing QR factorization.^{22,23} Such a factorization computes $A \Pi = Q[R_1 \ R_2]$, where Q is an $N \times k$ orthonormal matrix, R_1 is an upper triangular matrix, and Π is a permutation matrix. The permutation Π is chosen to keep R_1 well-conditioned. The interpolative decomposition is a powerful technique, and it can be used to build low-rank approximations for a matrix A with many small singular values (i.e., A has many columns that are almost linearly dependent). In such cases, algorithms for constructing

these factorizations often choose k to ensure that a certain relative accuracy in the approximation of A is achieved. However, in our situation, we know P is exactly of rank N_e and are thus not concerned with approximation error.

It may not be feasible to compute an interpolative decomposition of P directly, because we would have to construct P explicitly. The storage cost of P is N^2 , and computing a partial rank revealing QR factorization of P scales as $O(N_e N^2)$, which is prohibitively expensive. Randomized algorithms exist that would reduce this cost, for example,^{24,25} but they do not achieve the desired computational scaling. To achieve the desired scaling, observe that, for any rank revealing QR factorization of Ψ^* ,

$$\Psi^* \Pi = QR$$

where Q is an $N_e \times N_e$ matrix with orthonormal columns, then

$$P \Pi = (\Psi Q) R$$

It can be readily verified that ΨQ is an $N \times N_e$ matrix with orthonormal columns. Therefore, rather than computing a rank revealing QR factorization of P , we may equivalently compute a rank revealing QR factorization of Ψ^* . This computation scales as $O(N_e^2 N)$. The permutation matrix Π reveals the selection of columns C , and the SCDM can be computed as

$$\tilde{\Phi} \equiv P_{:,c} = \Psi \Psi_{:,c}^*$$

Using the SCDM we may recover the density matrix in a simple manner. Since P is a rank N_e Hermitian, and positive semidefinite matrix, and $P_{:,c}$ has linearly independent columns, we may write P in the form $P = P_{:,c} D P_{:,c}^*$, where D is an $N_e \times N_e$ matrix. By restricting P to the C row and column indices, $P_{c,c} = P_{c,c} D P_{c,c}^*$, we observe that $D = (P_{c,c})^{-1}$ is uniquely determined. Therefore,

$$P = P_{:,c} (P_{c,c})^{-1} P_{:,c}^* \quad (4)$$

Equation 4 also suggests a method for the construction of orthonormal and localized basis functions. If we let

$$P_{c,c} = LL^*$$

be a Cholesky factorization of $P_{c,c}$, then

$$\Phi = \tilde{\Phi} L^{-*}$$

has orthogonal columns and they may be used as a basis for the span of Ψ . In this case we may also write $P = \Phi \Phi^*$. The orthogonality of Φ follows from P being an orthogonal projector. Based on the locality of the columns of P and because the permutation Π picks columns of P that form a well-conditioned basis, $P_{c,c}$ decays rapidly, exponentially given our assumptions on P , away from the diagonal. Consequently, for the systems that we consider, the orthogonalization step will not significantly impact the localization of the basis functions.

Coincidentally, we construct the SCDM $\tilde{\Phi}$ or the orthogonalized SCDM Φ via the algorithm below.

- (1) Compute the index set C associated with an interpolative decomposition of Ψ^* via a rank revealing QR decomposition.
- (2) Compute the SCDM $\tilde{\Phi} = P_{:,c} = \Psi(\Psi_{:,c})^*$ as the new localized basis. If the orthogonalized SCDM are desired, then

(3) Compute the Cholesky factorization $P_{c,c} = LL^*$

(4) Compute the orthogonal basis Φ by solving $\Phi L^* = \tilde{\Phi}$

This algorithm is completely deterministic and can be applied to any local or nonlocal basis set. In general, when computing the rank revealing QR factorization for an interpolative decomposition, a so-called strong rank revealing QR factorization is technically required. However, for the types of systems that we are interested in, a more traditional rank revealing QR factorization, such as the one implemented in LAPACK²⁶ as DGEQP3, suffices. The use of a Cholesky factorization allows us to avoid explicit inversion of $P_{c,c}$ and, instead, use triangular solves to either apply the spectral projector or orthogonalize the basis.

The overall cost of the algorithm is $O(N_e^2 N + N_e^3)$ to build Φ or $\tilde{\Phi}$. The cost of the necessary rank revealing QR is $O(N_e^2 N)$ and the dominant cost in N_e that has no dependence on N is the Cholesky factorization, which costs $O(N_e^3)$. The cost of forming the columns of $\tilde{\Phi}$ is $O(N_e^2 N)$, as is the cost of constructing Φ via triangular solves. Because the algorithm is constructed from simple and standard linear algebra routines, it is easy to parallelize. Specifically, steps 1, 2, and 4 in the preceding algorithm may each use a parallel version (e.g., from ScaLAPACK)²⁷ of the respective linear algebra routine. Because the required Cholesky factorization is of a $N_e \times N_e$ matrix, it is often not necessary to parallelize that portion of the algorithm, although one certainly could. By utilizing common factorizations and operations, the algorithm immediately benefits from improvements to the underlying, serial or parallel, linear algebra routines and does not require any specialized code. One example of this would be the use of recent variants for computing a parallel rank revealing QR factorizations such as the communication avoiding version discussed in ref 28. The efficiency of a parallel version will be briefly discussed in the Numerical Results section.

To illustrate the simplicity of the algorithm, we present a serial implementation of the algorithm in MATLAB.²⁹ The following two lines of code implement the above algorithm and compute the SCDM. The discrete input Ψ , which has orthonormal columns, is represented as `Psi` and `Ne` is the column dimension of Ψ , and therefore the number of localized basis functions. When complete, the matrix `Pc` contains the localized SCDM.

```
[Q, R, piv] = qr(Psi', 0);
Pc = Psi*(Psi(piv(1:Ne), :)');
```

If a set of orthonormal and localized orbitals are to be computed, the following three lines can be added, and the matrix `Phi` contains the orthogonalized and localized SCDM.

```
S = Pc(piv(1:Ne), :);
Rchol = chol(S);
Phi = Pc/(Rchol);
```

3. NUMERICAL RESULTS

3.1. Localized Basis Functions. We now demonstrate the effectiveness of our algorithm from both qualitative and quantitative points of view. For all of our numerical experiments, we used QUANTUM ESPRESSO³⁰ to compute the eigenfunctions. The SCDM are then computed from the Kohn–Sham orbitals for the occupied states.

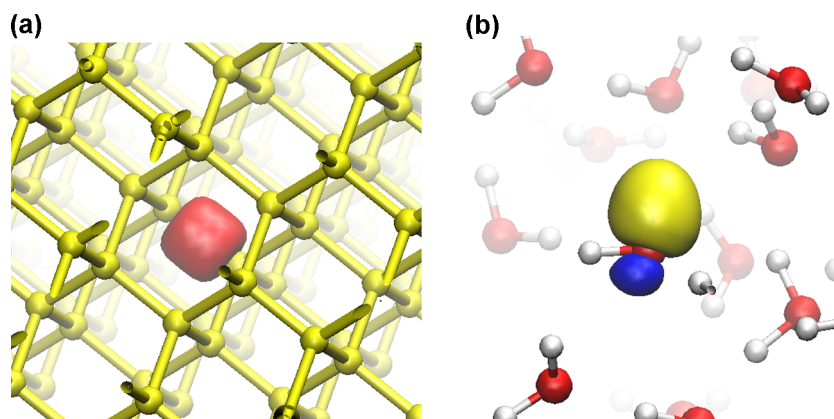


Figure 1. Isosurface for an orthogonalized SCDM for (a) a silicon crystal with 512 Si atoms (yellow balls) and (b) a water system with 64 O atoms (red balls) and 128 H atoms (white balls). In panel (a), the red isosurface (at a value of 0.029 a.u.) characterizes the orthogonalized SCDM located between two Si atoms. In panel (b), the yellow and blue isosurfaces characterize the positive (at a value of 0.008 a.u.) and negative (at a value of -0.008 a.u.) portions of the orthogonalized SCDM, respectively.

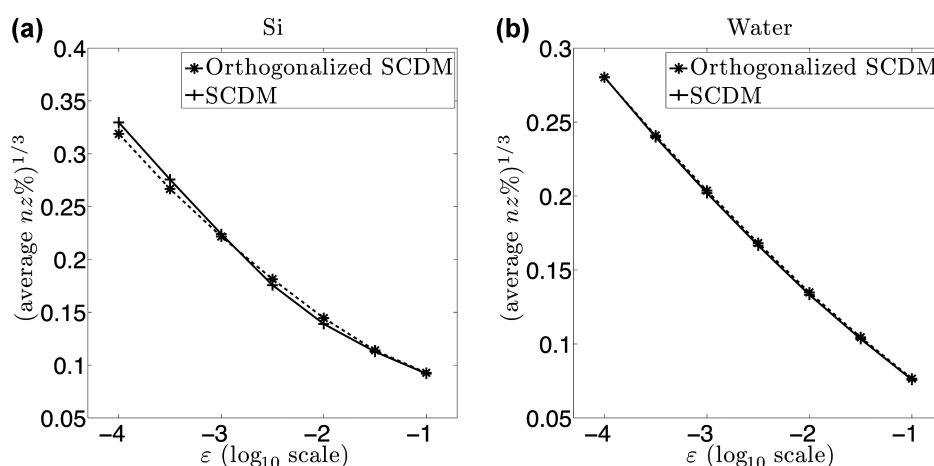


Figure 2. Average fraction of nonzero entries after truncation for the SCDM and the orthogonalized SCDM for (a) the 512-atom silicon crystal and (b) 64 water molecules.

We first demonstrate the method qualitatively by computing localized basis functions for two different three-dimensional systems. Figure 1a shows one of the orthogonalized SCDM obtained from a silicon crystal with 512 atoms consisting of $4 \times 4 \times 4$ unit cells with diamond structure, and the dimension of each unit cell is $10.26 \text{ a.u.} \times 10.26 \text{ a.u.} \times 10.26 \text{ a.u.}$ Figure 1b shows one of the orthogonalized SCDM obtained from a water system with 64 molecules in a cubic supercell with dimensions of $22.08 \text{ a.u.} \times 22.08 \text{ a.u.} \times 22.08 \text{ a.u.}$, which corresponds to a density of 1.2 g/cm^3 . The kinetic energy cutoff for the silicon crystal is 10 Ry, and for water is 75 Ry. For all calculations, we use the Troullier–Martins pseudo-potential³¹ with the Perdew–Burke–Ernzerhof (PBE) functional.³² The orbitals are very localized in the real space and resemble the shape of MLWFs.⁶ In fact, in this case, our method automatically finds the centers of all localized orbitals, which, for the silicon crystal, are in the middle of the Si–Si bond, and, for water, is closer to the oxygen atoms than to the hydrogen atoms.

The locality of the SCDM is demonstrated by computing the fraction of entries, averaged across all N_e localized functions, that remain nonzero (denoted by $nz\%$) after truncating each basis function below a certain relative threshold (denoted by ϵ). The diameter of the localized region is proportional to the cubic root of the volume and, thus, is proportional to $(nz\%)^{1/3}$.

Exponential decay implies that $\exp[-C(nz\%)^{1/3}] \approx \epsilon$, where C is a constant independent of ϵ . Therefore, exponentially localized orbitals should manifest themselves as a straight line when $(nz\%)^{1/3}$ is plotted on a linear scale, and ϵ is plotted on a log-scale. Figure 2 shows such a relation for the SCDM basis functions, both before and after orthogonalization, as the relative truncation threshold is varied.

When the relative truncation value is 10^{-2} , the average fraction of nonzero entries of each localized basis function is roughly 0.3% for both the 512-atom silicon crystal and the 64 water molecules, thereby significantly reducing the storage cost for the orbitals. We note that the orthogonalization procedure does not significantly impact the locality of the functions, although, generally, we do not expect this procedure to result in more localized functions. The good localization properties also imply that $P_{c,c}$ should be a well-conditioned matrix. In fact, we observe that the condition number is only 3.18 for the silicon crystal and 2.83 for the water molecules.

3.2. Computation of Hartree–Fock Exchange Energy.

We now use the orthogonalized SCDM to compute the Hartree–Fock exchange energy with, under some mild assumptions, linear scaling cost. The Hartree–Fock exchange energy is invariant under unitary transformation of the Kohn–Sham orbitals, and can be computed as

$$E_x = -\frac{1}{2} \sum_{i,j=1}^{N_e} \iint \frac{\phi_i(x)\phi_j(x)\phi_j(y)\phi_i(y)}{|x-y|} dx dy \quad (5)$$

Here, $\{\phi_i\}_{i=1}^{N_e}$ can be the Kohn–Sham orbitals, or any unitary transformation of them. We remark that for periodic systems the Coulomb integral in the Fourier basis should be treated with care. In this manuscript, we use $4\pi/G^2(|G| \neq 0)$ as the Coulomb kernel in the Fourier basis for simplicity, where \mathbf{G} is a reciprocal lattice vector. We refer readers to, for example, ref 33 for more-detailed discussion on the comparison of different Coulomb kernels for periodic systems. Note that the efficiency of the algorithm here is not affected by specific choices of Coulomb kernels.

When eq 5 is computed using the Kohn–Sham orbitals $\{\psi_i\}_{i=1}^{N_e}$ directly the standard method is to use the plane-wave basis set and solve Poisson’s equation for each pair of Kohn–Sham orbitals. This results in having to solve $O(N_e^2)$ discrete versions of Poisson’s equation with periodic boundary conditions and enforcing zero mean in the solution, which may be done via use of the Fast Fourier Transform (FFT). The overall cost for computing the energy is then $O(N_e^2 N \log N)$, where the $\log N$ factor arises from the FFT. In a hybrid functional calculation such as PBE0 functionals³ the cost of this step can be dominating, compared to a calculation using semilocal exchange–correlation functionals.

By using the orthogonalized and truncated SCDM instead of the delocalized Kohn–Sham orbitals, the computational cost can be significantly reduced, at the expense of introducing some controllable error. Let $\hat{\Phi} = [\hat{\phi}_1, \dots, \hat{\phi}_{N_e}]$ denote the truncated version of Φ . This truncation introduces some error, but the relative truncation value may be chosen to achieve any desired accuracy. After truncation, we may simply neglect pairs of $\hat{\phi}_i$ and $\hat{\phi}_j$ with disjoint support, or if their product is sufficiently small on the global domain. The latter criteria for neglecting pairs may even be done without truncating the basis functions to explicitly make their representations sparse. When each $\hat{\phi}_i$ is localized the $O(N_e^2)$ terms in eq 5 is reduced to $O(N_e)$ significant terms. In fact, this reduction in the number of times that the Poisson’s equation needs to be solved provides substantial computational savings on its own. For example, for the 64-water-molecule system, Figure 3 shows the fraction of significant pairwise interactions, measured as the fraction of unique i, j pairs for which $\|\phi_i\phi_j\|_1 \geq \epsilon$. Note that, by convention, we have normalized ϕ such that $\|\phi_i\phi_j\|_1 = 1$.

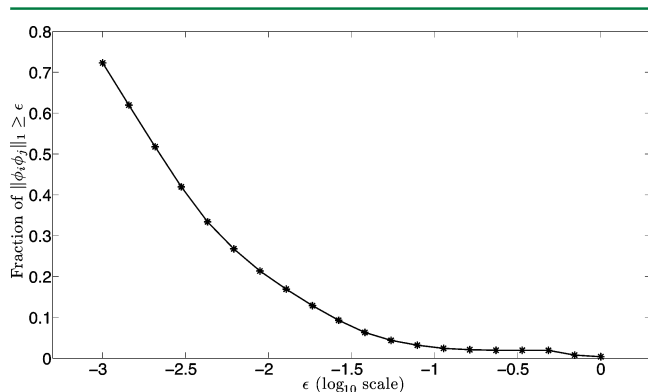


Figure 3. Fraction of unique i, j pairs where $\|\phi_i\phi_j\|_1 \geq \epsilon$ with the localized basis functions computed for the 64-water-molecule system.

If the functions have been explicitly truncated, the computational cost can be further reduced by noting that the solution of Poisson’s equation is only needed on the support of $\hat{\phi}_i\hat{\phi}_j$. This fact may be used to reduce the size of each FFT by using Hockney’s algorithm.^{34,35} Hockney’s algorithm is a fast and direct method that does not introduce any additional approximation error. A brief presentation of the main idea of Hockney’s method is provided in the Supporting Information.

Given the above techniques we still have to determine the support of $\hat{\phi}_i\hat{\phi}_j$ for all i, j pairs, which scales as $O(N_e^2)$. However, if the vectors are appropriately stored, this operation amounts to a few logical operations per pair of $\hat{\phi}$ and will not be a dominant portion of the computational cost. Ignoring this cost and assuming that, as the number of atoms and size of a molecule grows, the support of the basis functions remains constant, yields an overall computational scaling of $O(N_e)$. Here, the constant will be dominantly dependent on the size of the FFTs required by Hockney’s algorithm.

To demonstrate the efficiency and accuracy of computing the Hartree–Fock exchange energy using the orthogonalized SCDM, we construct a quasi one-dimensional silicon crystal extended along the z -direction. The total number of atoms varies from 32 to 512, and, for each problem size, N_e is twice the number of atoms. The kinetic energy cutoff and other parameters are the same as for the aforementioned silicon crystal. All calculations are performed on a single computational node. Figure 4 shows the time to compute the Hartree–Fock exchange energy when using the localized and truncated basis functions. Our error criteria is the relative error in the computed exchange energy. We truncate the localized basis

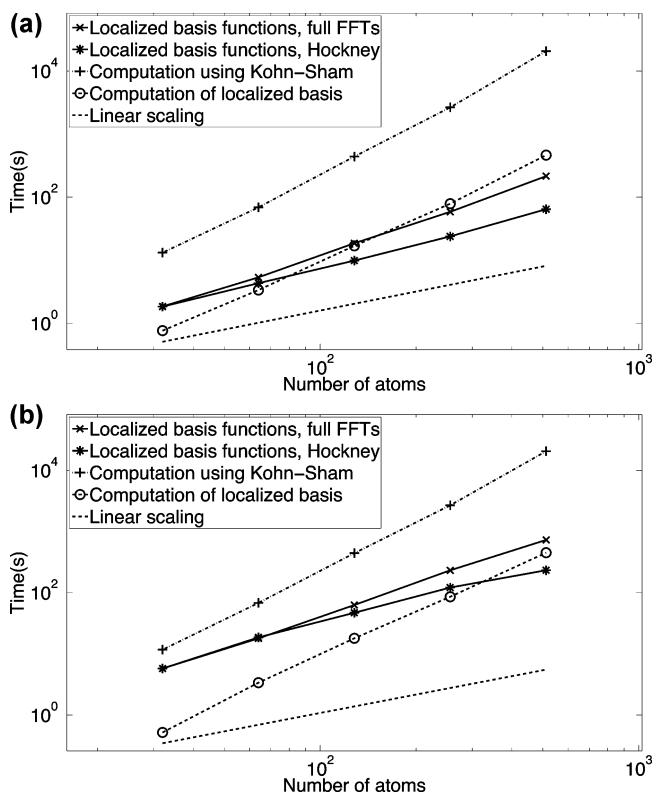


Figure 4. Time to compute the Hartree–Fock exchange energy and the localized basis functions. The localized basis functions were truncated to achieve (a) 4%–5% and (b) 0.3%–0.4% relative error in the energy computation.

functions at two different values, and achieve relative error of 4%–5% in Figure 4a and 0.3–0.4% in Figure 4b. Table 1

Table 1. Comparison of the Per Atom Exchange Energy Computed Using the Kohn–Sham Orbitals with the Approximation Computed by Localizing the Basis Functions, Truncating Them, and Neglecting Terms of the Sum in eq 5^a

| number of atoms | exchange energy per atom (a.u.) | computed energy per atom (a.u.) | error per atom (a.u.) |
|-----------------|---------------------------------|---------------------------------|-----------------------|
| 32 | −0.5626 | −0.5607 | 0.0019 |
| 64 | −0.9667 | −0.9635 | 0.0031 |
| 128 | −1.7811 | −1.7752 | 0.0059 |
| 256 | −3.4130 | −3.4011 | 0.0119 |
| 512 | −6.6782 | −6.6541 | 0.0241 |

^aThe artificial increase of the exchange energy per atom, with respect to the increase of the system size, is due to our use of $4\pi/G^2(|G| \neq 0)$ as the Coulomb kernel in the Fourier basis.

shows, for the scenario where a relative error of 0.3–0.4% was achieved, the computed exchange energy per atom using Kohn–Sham orbitals, the approximation computed by truncating the localized basis functions and neglecting terms of the sum in eq 5, and the absolute error.

We observe that using the localized and truncated functions greatly reduces the computational time, even when factoring in the cost of performing the localization to obtain the orthogonalized SCDM. The cost for the localization scales as $O(NN_e^2)$ but is more than an order of magnitude faster (even more so if a parallel version is used) than computing the exchange energy directly using Kohn–Sham orbitals. It is also clear that the use of localized basis functions without using Hockney’s algorithm (“full FFTs”) reduces the observed computational cost to $O(NN_e \log N)$, while using Hockney’s algorithm (“Hockney”) further reduces the computational cost to $O(N_e)$. For the largest problem size, the acceleration in computing the exchange energy using the localized basis functions and Hockney’s algorithm relative to the computational time using Kohn–Sham orbitals is a factor of ~ 300 when the relative error is 4%–5%, and a factor of 90 when the relative error is 0.3%–0.4%.

3.3. Parallel Computation. The above discussion featured results for the localization procedure and the subsequent computation of the Hartree–Fock exchange energy when using a single machine. For the largest quasi one-dimensional problem considered, Ψ is a 777600×1024 matrix. To demonstrate how the algorithm may be parallelized, we implemented a simple parallel version in FORTRAN using ScaLAPACK²⁷ for the parallel rank-revealing QR. The pivoted QR, the matrix multiplication to form $\hat{\Phi}$, and the triangular solve to form Φ were all done using parallel versions of the respective algorithms. We make note of the fact that the parallel timings given here are not on machines of the same type as those used previously for the examples, so the absolute times are not directly comparable. Computing the orthogonalized SCDM for the aforementioned problem using this code and 1024 processors took less than 1.5 s. This is not including the time to distribute Ψ among the processors, which took 1.3 s, nor the time to read Ψ from disk. In Figure 5, we show the scaling of this parallel implementation for computing the orthogonalized SCDM. Once again, we omit the time taken to

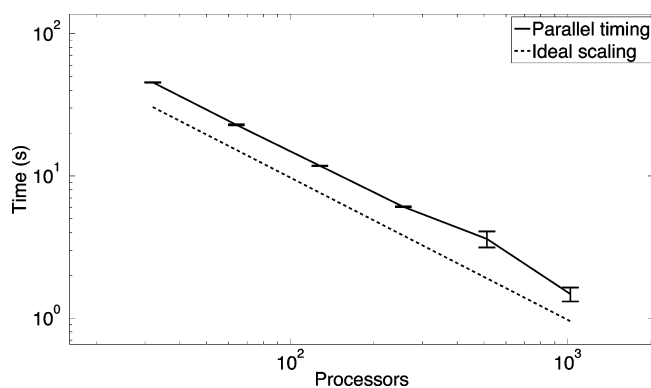


Figure 5. Parallel scaling for computing the orthogonalized SCDM. The times given are the average over 10 computations, and the error bars are one standard deviation away from the mean.

distribute the matrix. Here, we see that, for the given problem size, the method scales almost ideally on up to 1024 processors.

4. CONCLUSION

We have presented a simple procedure to obtain compressed Kohn–Sham orbitals by directly using selected columns of the density matrix (SCDM). The nearsightedness principle guarantees the locality of the SCDM for insulating systems. The computation of the orthogonalized SCDM is a simple and fast procedure that may be done immediately following the computation of Ψ to build a well-localized orthogonal basis for the Kohn–Sham orbital subspace. Because the algorithm is built out of a few very simple linear algebra routines, it is simple to implement, parallelize, and include in electronic structure software packages.

Our work can be extended in several directions. Besides the computation of the Hartree–Fock exchange energy, the high parallel scalability of the SCDM procedure can enable the computation of localized basis functions for the self-consistent treatment of the Hartree–Fock exchange terms in Kohn–Sham density functional theory (KSDF) calculations with hybrid functionals.

In this work, we explicitly require the Kohn–Sham orbitals to be represented on a real space grid. This is very natural for electronic structure software packages based on planewave and finite difference methods, but may or may not be natural for other basis sets such as localized atomic orbitals. In fact, the locality of the single particle density matrix along the off-diagonal direction generally holds when the density matrix is represented using localized basis functions.¹⁷ Therefore, it would be possible to directly find the localized representation of the single particle density matrix represented using localized basis functions and skip the real-space representation. The numerical consequence of this procedure should be carefully tested.

The cost of computing the SCDM may be reduced via a randomized version of the algorithm. For the examples presented here, this method slightly reduced the quality of the localized basis functions and, consequently, was not used. However, it may still be beneficial for very large problems. The SCDM may also be a useful tool for achieving linear scaling electronic structure calculations for insulating systems, as well as higher-level quantum chemical treatment at the post-DFT level. Our idea is not limited to the compression of Kohn–Sham orbitals, but may also be generalized for the compression

of pair products of Kohn–Sham orbitals in excited-state calculations.

■ ASSOCIATED CONTENT

● Supporting Information

A brief overview of Hockney's algorithm is provided as Supporting Information. This material is available free of charge via the Internet at <http://pubs.acs.org/>.

■ AUTHOR INFORMATION

Corresponding Author

*E-mail: damle@stanford.edu.

Notes

The authors declare no competing financial interest.

■ ACKNOWLEDGMENTS

This work is partially supported by NSF Fellowship No. DGE-1147470 (A.D.) and NSF Grant No. DMS-0846501 (A.D. and L.Y.); by a Simons Graduate Research Assistantship (A.D.); by the DOE Scientific Discovery through Advanced Computing (SciDAC) program, and the DOE Center for Applied Mathematics for Energy Research Applications (CAMERA) program (L.L.); and by the Mathematical Multifaceted Integrated Capability Centers (MMICCs) effort within the Applied Mathematics activity of the U.S. Department of Energy's Advanced Scientific Computing Research program, under Award No. DE-SC0009409 (L.Y.). We thank Lenya Ryzhik and the National Energy Research Scientific Computing (NERSC) center for providing the computational resources. We are grateful to Wibe de Jong and Eric Bylaska for valuable suggestions to improve our manuscript.

■ REFERENCES

- (1) Hohenberg, P.; Kohn, W. *Phys. Rev.* **1964**, *136*, B864–B871.
- (2) Kohn, W.; Sham, L. *Phys. Rev.* **1965**, *140*, A1133–A1138.
- (3) Perdew, J. P.; Ernzerhof, M.; Burke, K. *J. Chem. Phys.* **1996**, *105*, 9982–9985.
- (4) Becke, A. D. *J. Chem. Phys.* **1993**, *98*, 5648.
- (5) Foster, J. M.; Boys, S. F. *Rev. Mod. Phys.* **1960**, *32*, 300.
- (6) Marzari, N.; Vanderbilt, D. *Phys. Rev. B* **1997**, *56*, 12847.
- (7) Marzari, N.; Mostofi, A. A.; Yates, J. R.; Souza, I.; Vanderbilt, D. *Rev. Mod. Phys.* **2012**, *84*, 1419–1475.
- (8) Gygi, F. *Phys. Rev. Lett.* **2009**, *102*, 166406.
- (9) E, W.; Li, T.; Lu, J. *Proc. Natl. Acad. Sci. U. S. A.* **2010**, *107*, 1273–1278.
- (10) Ozoliņš, V.; Lai, R.; Cafisch, R.; Osher, S. *Proc. Natl. Acad. Sci. U. S. A.* **2013**, *110*, 18368–18373.
- (11) Kohn, W. *Phys. Rev. Lett.* **1996**, *76*, 3168–3171.
- (12) Prodan, E.; Kohn, W. *Proc. Natl. Acad. Sci. U. S. A.* **2005**, *102*, 11635–11638.
- (13) Goedecker, S. *Rev. Mod. Phys.* **1999**, *71*, 1085.
- (14) Bowler, D. R.; Miyazaki, T. *Rep. Prog. Phys.* **2012**, *75*, 036503.
- (15) Wu, X.; Selloni, A.; Car, R. *Phys. Rev. B* **2009**, *79*, 085102.
- (16) Gygi, F.; Duchemin, I. *J. Chem. Theory Comput.* **2012**, *9*, 582–587.
- (17) Benzi, M.; Boito, P.; Razouk, N. *SIAM Rev.* **2013**, *55*, 3–64.
- (18) Blount, E. In *Formalisms of Band Theory*; Seitz, F., Turnbull, D., Eds.; Solid State Physics, Vol. 13; Academic Press: New York, 1962; pp 305–373.
- (19) Cloizeaux, J. D. *Phys. Rev. A* **1964**, *135*, A685–A697.
- (20) Cloizeaux, J. D. *Phys. Rev. A* **1964**, *135*, A698–A707.
- (21) Nenciu, G. *Comm. Math. Phys.* **1983**, *91*, 81–85.
- (22) Cheng, H.; Gimbutas, Z.; Martinsson, P.; Rokhlin, V. *S.I.A.M. J. Sci. Comput.* **2005**, *26*, 1389–1404.
- (23) Gu, M.; Eisenstat, S. *S.I.A.M. J. Sci. Comput.* **1996**, *17*, 848–869.
- (24) Martinsson, P. G.; Rokhlin, V.; Tygert, M. *Appl. Comput. Harmon. Anal.* **2011**, *30*, 47–68.
- (25) Liberty, E.; Woolfe, F.; Martinsson, P. G.; Rokhlin, V.; Tygert, M. *Proc. Natl. Acad. Sci. U. S. A.* **2007**, *104*, 20167–20172.
- (26) Anderson, E.; Bai, Z.; Bischof, C.; Blackford, S.; Demmel, J.; Dongarra, J.; Du Croz, J.; Greenbaum, A.; Hammarling, S.; McKenney, A.; Sorensen, D. *LAPACK Users' Guide*, 3rd Edition; Society for Industrial and Applied Mathematics (SIAM): Philadelphia, PA, 1999.
- (27) Blackford, L. S.; Choi, J.; Cleary, A.; D'Azevedo, E.; Demmel, J.; Dhillon, I.; Dongarra, J.; Hammarling, S.; Henry, G.; Petitet, A.; Stanley, K.; Walker, D.; Whaley, R. C. *ScaLAPACK Users' Guide*; Society for Industrial and Applied Mathematics (SIAM): Philadelphia, PA, 1997.
- (28) Demmel, J. W.; Grigori, L.; Gu, M.; Xiang, H. *S.I.A.M. J. Matrix Anal. Appl.* **2015**, *36*, 55–89.
- (29) *MATLAB, version 7.11.0 (R2010b)*; The MathWorks, Inc.: Natick, MA, 2010.
- (30) Giannozzi, P.; Baroni, S.; Bonini, N.; Calandra, M.; Car, R.; Cavazzoni, C.; Ceresoli, D.; Chiarotti, G. L.; Cococcioni, M.; Dabo, I.; Dal Corso, A.; de Gironcoli, S.; Fabris, S.; Fratesi, G.; Gebauer, R.; Gerstmann, U.; Gougoussis, C.; Kokalj, A.; Lazzeri, M.; Martin-Samos, L.; Marzari, N.; Mauri, F.; Mazzarello, R.; Paolini, S.; Pasquarello, A.; Paulatto, L.; Sbraccia, C.; Scandolo, S.; Sclauzero, G.; Seitsonen, A. P.; Smogunov, A.; Umari, P.; Wentzcovitch, R. M. *J. Phys.: Condens. Matter* **2009**, *21*, 395502.
- (31) Troullier, N.; Martins, J. L. *Phys. Rev. B* **1991**, *43*, 1993–2006.
- (32) Perdew, J. P.; Burke, K.; Ernzerhof, M. *Phys. Rev. Lett.* **1996**, *77*, 3865–3868.
- (33) Bylaska, E. J.; Tsemekhman, K.; Baden, S. B.; Weare, J. H.; Jonsson, H. *J. Comput. Chem.* **2011**, *32*, 54–69.
- (34) Hockney, R. W. *J. Assoc. Comput. Mach.* **1965**, *12*, 95–113.
- (35) Eastwood, J. W.; Brownrigg, D. R. K. *J. Comput. Phys.* **1979**, *32*, 24–38.